Fabrication, characterization and modelling of multilayered cantilevers with piezoelectric AlN ceramic as actuator.

A. Andrei[1], K. Krupa[1], P. Delobelle[2*], L. Hirsinger[2], C. Gorecki[1], L. Nieradko[1]

[1] LOPMD, FEMTO-ST, 16 Route de Gray, 25000 Besancon, France
[2] LMARC, FEMTO-ST, 24 Chemin de l'Epitaphe, 25000 Besancon, France
** Email: patrick.delobelle@univ-fcomte.fr*

Abtract :

This paper treats a wide range of subjects related to the use of AlN as actuation layer in MEMS, from its deposition conditions to accurate interferometric device characterization and physical parameter extraction. Parameters concerning the AlN films such as Young's modulus, residual thin film stresses, thermal expansion coefficient α and piezoelectric coefficient d_{31} have been calculated using non approximated equations capable of taking into account multiple film stacking(electrode/AlN/electrode/Si substrate).

Résumé :

Ce papier présente les potentialités de films d'AlN piézoélectriques comme éléments actionneurs pour les MEMS. Le cas de micro-poutres constituées d'un empilement de différents films (electrode/AlN/electrode/ substrat de Si) est présenté. Un dispositif interferométrique de type Twyman-Green permet de quantifier précisément les déformées et les déplacements ce qui permet de calculer différentes grandeurs physiques des films d'AlN, par exemple le module d'Young, les contraintes résiduelles liées à l'élaboration, le coefficient de dilatation α ainsi que le coefficient piézoélectrique d_{31} .

Key-words: Piezoelectric; AlN ceramic ; cantilevers

1 Introduction

Aluminium nitride (AlN) films have piezoelectric properties that are already used for acoustic wave propagation in miniature high frequency bypass filters for the ever-growing wireless communication market, J.H. Kim *et al*. (2002), K.M. Lakin *et al.* (2001). This is a promising material also for MEMS applications and sensors using surface acoustic waves have already been proposed, A. Choujaa *et al*. (1995), T. Laurent *et al*. (2000). For actuation purposes, even if PZT films are most of the time used for their better piezoelectric properties, H.P. Löbl *et al*. (1999), AlN still represents an alternative that has been explored, D. Ruffieux *et al*. (2000). The objective of the present work is to develop high quality AlN cantilevers that will serve as reliable actuation elements in more complex MEMS. After presenting the fabrication process of the AlN driven cantilevers, the rest of the paper will focus on these device characterization and physical parameter extraction.

2 Experimental work

2.1 Sample fabrication

The AlN driven micro-beams were fabricated on 380 µm thick, 3'' (100) oriented Si wafers. The process flow is shown in Fig.1. After realizing a 15 µm thick Si membrane by KOH etch of bottom side of the wafer (step 1), on the top side are successively deposited three thin layers: two CrNi PVD metal layers (0.15 µm at step 2 and 0.35 µm at step 4) that have between

them the AlN film. The $Cr_{50\%}Ni_{50\%}$ alloy has been sputtered on a heated substrate (200°C) at 230 watt (0.5 A) using a 0.93 Pa Ar gas. The AlN has been deposited (step 3) in a pulsed reactive DC sputtering machine on a non heated substrate with an input power of 650 watt, a Ar / N_2 gas ratio of 0.65 sccm / 6 sccm and a pressure of 0.65 Pa. These conditions led to a deposition rate around 17 nm /mn. Two different wafers have been processed, having a final AlN thickness of 1 µm and 1.4 µm. The top CrNi electrode patterned at step 4, has been used as a hard mask during AlN and silicon etching (steps 5 and 7). An intermediary process step allowed the deposition and patterning of 0.5 µm thick Aluminium pads that were used for wire bonding. The last RIE step removed the silicon which was not protected by the CrNi hard mask, transforming the initial Si membranes into an array of free standing cantilevers. They had a constant width of 50 µm and variable lengths from 200 µm up to 900 µm. The layout of the cantilever array is shown in Fig.2.

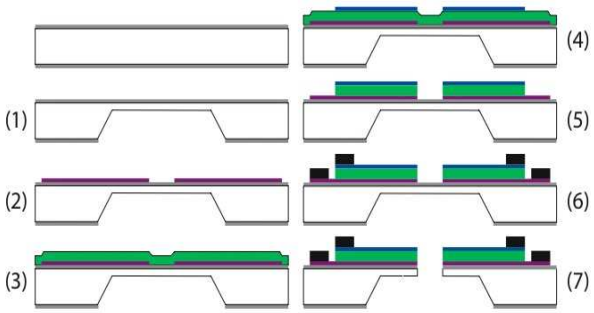

Fig.1 : Cantilever process flow chart.

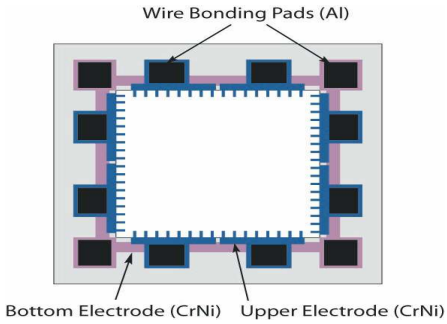

Fig.2 : Layout of the 200 µm long cantilevers.

Prior the fabrication of the devices, a series of test structures has been realized. They allowed the measurement of the stress in the films and the influence of the bottom electrode nature over the stress in the AlN film. These test structures were arrays of 13 µm thick silicon cantilevers, 5 mm wide, width lengths varying from 0.5 mm up to 3.5 mm. Two bottom electrodes have been tested: 0.16 µm thick CrNi and 0.24 µm thick Pt films. The CrNi has been deposited using the same conditions that for the devices, while the Pt has been sputtered on a non biased , non heated substrate at 120 watt (0.22 A) using a 1.1 Pa Ar gas. After measuring the cantilever bending, a 0.8 µm thick AlN layer has been deposited using the same conditions that for the devices.

2.2 AlN Young's modulus measurement

Nano-indentation tests were performed on the AlN films of the test structures using a nanoindenter II^S with a Berkovich tip. The study was conducted following the continuous contact stiffness measurement procedure, W.C. Oliver *et al*. (1992), with a frequency of 45 Hz and a indenter vibration amplitude of 1 nm during the penetration of the tip into the sample. It allowed the determination of the $M_{<hkl>}$ modulus for AlN deposited on Pt and CrNi electrodes.

2.3 Cantilever deflection measurement

Both test structures as the AlN driven cantilevers have been characterized using a previously validated measurement set-up based on a Twyman-Green interferometer, C. Gorecki *et al*. (2005), L. Salbut *et al*. (2003). Five frames of interferometric intensity data taken at 90° relative phase shifts (Fig.3 shows an example of such interferograms) are used with a phase shifting algorithm in order to obtain a highly accurate (20 nm accuracy on vertical displacement) measurement of the cantilever profile. Fig.4 shows such a measured profile of three 800 µm adjacent cantilevers. This experimental set-up allowed both static and dynamic

measurements of the samples. The use of a Thermal Control Modulus allowed us to fix the sample temperature anyway between 15°C and 60°C with 0.01°C accuracy

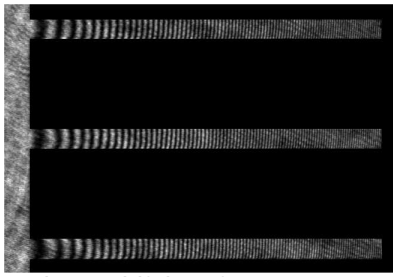

Fig.3 : 5 phase shift interferograms used for the cantilever profile calculation.

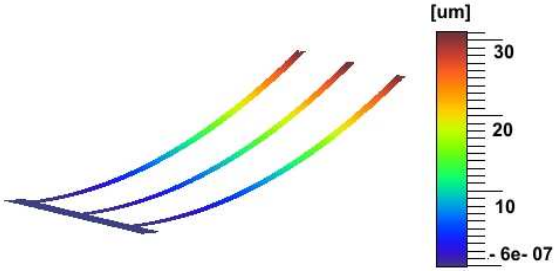

Fig.4: 3D view of the measured profile for 800 µm long cantilevers.

3 Equations for multilayered cantilevers

The use of the same metal (CrNi) for the top and bottom electrodes, allows us to consider for simplification reasons that the silicon cantilever has on its surface only two films: the AlN film and a metal electrode film with a thickness equal to the sum of the top and bottom electrodes thicknesses. The stress in the AlN and metal films are causing a mechanical deflection δ_m of the three layers cantilevers that can be written as, Q.M. Wang *et al*. (1999), V. Walter (2001):

$$\delta_m = \frac{3(1-\upsilon)}{E_{eq}h_{eq}^2}\,\frac{E_s h_s^2 - (E_f h_f + E_e h_e)(h_e + h_f)}{E_s h_s + E_f h_f + E_e h_e} L^2 \sigma_0 \qquad (1)$$

with the global stress σ_0 :

$$\sigma_0 = \frac{\sigma_f h_f + \sigma_e h_e + \sigma_s h_s}{h_{eq}} \qquad (2)$$

where E_i, h_i and σ_i with i = s, f, e are the Young Modulus, the thickness and the stress of the silicon substrate (s), the AlN film (f) and the metal electrodes (e). L represents the cantilever's length and υ the Poisson coefficient considered the same for all the materials. The equivalent thickness h_{eq} is equal to the sum of h_s, h_f, and h_e, while E_{eq} represents the equivalent modulus that can be written as:

$$E_{eq} = \frac{K_1 + K_2 + K_3 + K_4 + K_5}{(E_f h_f + E_s h_f + E_e h_e) h_{eq}^3} \quad \text{with:} \quad K_1 = E_f^4 h_f^4 + E_s^4 h_s^4 + E_e^4 h_e^4$$

$$K_2 = 2E_s E_e h_s h_e (2h_s^2 + 2h_e^2 + 3h_s h_e) \qquad K_3 = 2E_f E_e h_f h_e (2h_f^2 + 2h_e^2 + 3h_f h_e) \qquad (3)$$

$$K_4 = 2E_f E_s h_f h_s (2h_s^2 + 2h_f^2 + 3h_s h_f) \qquad K_5 = 12 E_s E_f h_s h_f h_e h_{eq}$$

Under an applied voltage V, the piezoelectric properties of the AlN film will cause an additional deflection δ_p that can be related to the AlN piezoelectric coefficient d_{31} by:

$$\delta_p = -\frac{3}{E_{eq}h_{eq}^2}\,\frac{E_f(E_s h_s + E_e h_e)}{E_s h_s + E_f h_f + E_e h_e} d_{31} L^2 V \qquad (4).$$

Under a thermal loading ΔT, the corresponding deflection δ_{Th} of the bender, function of the thermal expansion coefficients of the three layers, α_e, α_f, α_s , is given by:

$$\delta_{Th} = 3\frac{\left[E_s h_s^2 - (E_f h_f + E_e h_e)(h_e + h_f)\right] x \left[\alpha_s (E_f h_f + E_e h_e) - (E_f \alpha_f h_f + E_e \alpha_e h_e)\right]}{E_{eq} h_{eq}^3 (E_f h_f + E_s h_s + E_e h_e)} L^2 \Delta T \qquad (5).$$

Putting in the above equations h_e=0 leads to the classic equations for a piezoelectric film deposited on a silicon cantilever, V. Walter *et al*.(2002). Furthermore, a first order development of the Eq.1 gives a generalized writing of the Stoney equation:

$$\sigma_f = \frac{E_s h_s^2 \delta_m}{3(1-\upsilon)h_f L^2}\left[1+\underbrace{4\frac{E_f h_f}{E_s h_s}}_{A}\left(1+\underbrace{\frac{3h_f}{2h_s}+\frac{h_f^2}{h_s^2}}_{B}\right)\right] \quad (6)$$

For our particular study, using the Stoney equation would have introduced a significant under-estimation of the stress in the film, since the values of the terms *A* and *B* are 0.97 and 0.11.

4 Results and discussion

4.1 Young's modulus and stress values

The indentation modulus $M_{<hkl>}$ for AlN was found to be dependent of the metal electrode on which the AlN film has been deposited: $M_{<hkl>}$ = 340 GPa for CrNi electrode for only $M_{<hkl>}$ = 290 GPa for the Pt electrode. Using the elastic constants C_{ij} for AlN films given in the literature, A.F. Wright *et al*. (1997), G. Carlotti *et al*. (1995), it can be shown that the value of $M_{<001>}$ is equal to 335 GPa (maximum value for $M_{<hkl>}$). Therefore, between the two metal electrodes that have been tested, the CrNi electrode proved to be the best choice since it led to a well (001) orientated AlN film. This observation is confirmed by the analysis of the X-rays diffraction spectrums which shows a perfectly (002) crystallites orientation for AlN on CrNi and a (002) orientation and amorphous part for AlN on Pt electrode.

Furthermore, the bending of the test structures cantilevers before and after the AlN deposition on their CrNi and respectively Pt electrodes, gave valuable information about the stress levels in the films. The measurements shown in Fig.5 indicated that the stress in the CrNi film is tensile, while the Pt film was under compression. The change of slope after AlN deposition indicates a compressive stress in this film. Numerical calculations using Eqs.1-3 led to values of +1110 MPa tension stress for CrNi and -700 MPa compressive stress for Pt. After its deposition on the two different metal electrodes, the stress value in the AlN film deposited on CrNi was of -220 MPa, versus -564 MPa for the one deposited on Pt. CrNi proved again to be a better choice as metal electrode since its allows the deposition of less stressed AlN. Moreover, if the thicknesses of the films are well chosen, it is possible to obtain a structure with a global stress equal to zero.

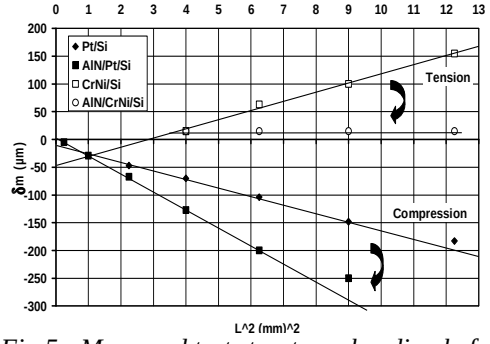

Fig.5: Measured test structures bending before and after AlN deposition as a function of their square length.

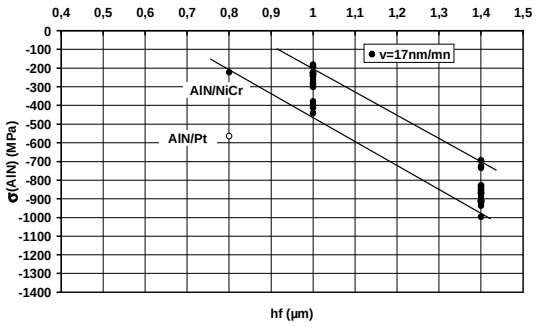

Fig.6: Calculated stress in the AlN films as a function of its thickness.

The compressive stress in the AlN film has been related in the literature to the high DC power input, K. Kusaka *et al*. (2000). W.J. Meng et al. (1993) have also shown that the stress was a function of the AlN film thickness: it had a minimum for thicknesses between 0.5 µm and 1.0 µm and it is increasing for greater thicknesses. These observations have been confirmed in our study. Fig.6 shows the calculated AlN stress in the test structures but also in the final devices that had AlN thicknesses of 1 µm (wafer1) and 1.4 µm (wafer 2). The AlN compressive stress is

significantly increasing with its thickness. Therefore, if the objective was to realize an AlN driven structure with low global stress, the CrNi electrodes thicknesses should be adjusted not only to the AlN thickness value, but also to its thickness depended stress value.

4.2 Piezoelectric coefficient determination

When a DC voltage is applied between the upper and the lower metal electrodes, a supplementary displacement δ_p (Eqs.3- 4) adds to the stress induced mechanical bending δ_m. As it is shown in Fig.7, the measured piezoelectric displacement δ_p showed a linear behaviour with the applied voltage. The slope for the wafer 2 samples is grater, since the AlN film is much thicker than for the wafer 1 devices (the Si and metal electrodes have the same thicknesses for both wafers). However, this different slope is not only related to the different thicknesses. Using Eq.4, the piezoelectric coefficient d_{31} value for wafer 2 (1.4µm AlN) was found to be -2.0 pm/V, for only -1.3 pm/V for the wafer 1 samples (1µm AlN). The first -2.0 pm/V value is in good agreement with d_{31} coefficients measured on pulsed reactive DC sputtered AlN films, I.L.Guy *et al*. (1999). However, for the wafer 1, the d_{31} value is somehow small, which indicates that the AlN deposition process needs further optimization.

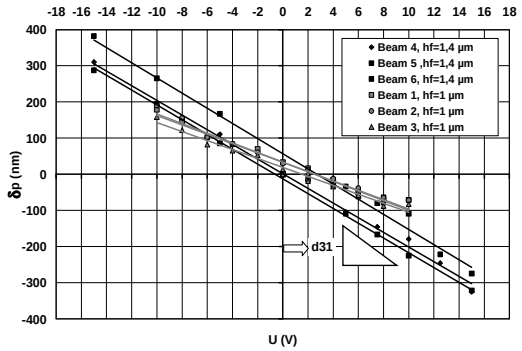

Fig.7: Determination of the d_{31} piezoelectric coefficient of the AlN films.

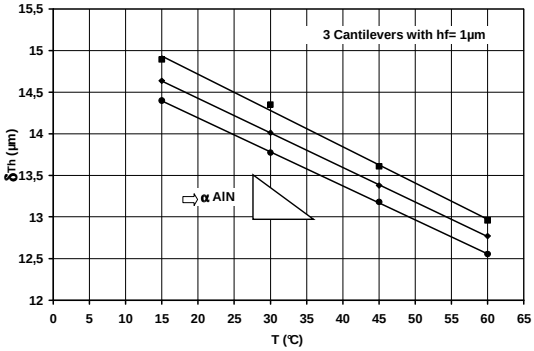

Fig.8: Determination of the thermal expansion coefficient α of the AlN films.

4.3 Thermal expansion coefficient determination

The Thermal Control Module allowed us to fix the cantilevers temperature between 15°C and 60°C and thus to determine the thermal expansion coefficient α of the AlN films (Eq.5). Fig.8 shows the variation of the total deflection $\delta_m + \delta_{Th}$ as a function of the temperature for three different beams. The application of Eq.5 knowing the slope of these curves ($\Delta\delta_{Th}/\Delta T$) and the material parameters (L = 800 µm, $\alpha_s = 2.44\ 10^{-6}\ K^{-1}$, $\alpha_e = 9.5\ 10^{-6}\ K^{-1}$) allowed us to calculate $\alpha_f = \alpha_{AlN}$. We found $4.3\ 10^{-6} < \alpha_{AlN} < 4.6\ 10^{-6}\ K^{-1}$, which is in good agreement with the values reported in the literature for bulk material; $4.4\ 10^{-6} < \alpha_{AlN} < 5.3\ 10^{-6}\ K^{-1}$.

4.4 Joule effect on some cantilevers

Impedance measurements R on all the wafer devices have been performed. They showed that some of the different cantilevers arrays present on each device were in short cut. When a voltage was applied to these cantilevers they had an important displacement $\delta >> \delta p$ proportional to the square of the voltage (Fig.9), that had a Joule effect origin. Note that 15 V applied bias proved to be too high for some of the cantilevers with h_f = 1 µm leading to severe damage of the electrodes and the AlN beneath it. After this damage it was observed important parabolic bending related to the heating of the AlN and Si films thanks to the electrodes.
From Fig.9, we can deduce the relation: $\delta_{Th}=A_{exp}V^2$ which combined with Eq.5 gives the relation $\Delta T= A^*_{exp}\ V^2$. A very simple thermal conduction model; a wall heated on one side by

an electric resistance, shows that: $\Delta T = \beta V^2 / R$ and thus $A^*_{exp} = \beta / R$. The representation $A^*_{exp} = f(1/R)$ for all the tested cantilevers in short cut (Fig.10) gives $120 < \beta < 190$ K/W.

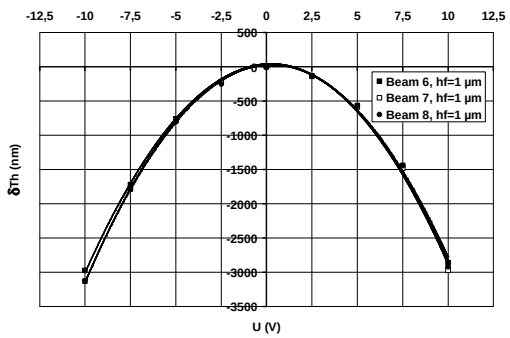

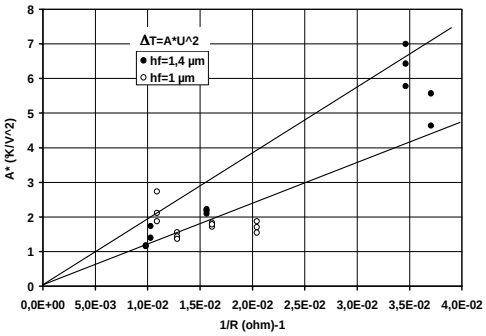

Fig.9: Responses with V^2 for the beams in short cut. Fig.10: Determination of the coefficient β.

4 Conclusions

The presented process allowed the fabrication of AlN driven cantilevers that have good piezoelectrical behaviour. CrNi proved to be a better choice as bottom electrode, since the AlN deposited on it had better (002) orientation, a well defined Young's modulus and lower stress. The influence of AlN thickness on its stress level has also been investigated, the obtained results being valuable information in designing AlN driven structures with a low global stress. The thermal expansion coefficient of these films has been determined. The devices obtained from the wafer with a thicker AlN film (1.4 µm) showed better piezoresistive properties, with a d_{31} coefficient of -2.0 pm/V. All the physical parameters have been calculated using non approximated analytical equations. From a material point of view, the important result is that the well oriented (002) AlN ceramic thin films exhibit approximately the same electro-thermo-mechanical properties, C_{ij}, α, $d_{31}{}^b$ as the bulk material.

References

Carlotti, G., Hickernell, F.S., Liaw, H.M., Palmieri, L., Socino, G. & Verona, E., 1995, *IEEE Ultrasonics Symposium*, 353-356.

Choujaa, A., Tirole, N., Bonjour, C., Martin, G., Hauden, D., Blint, P., Cachard, A. & Pommier, C., 1995, *Sensors and Actuators* A, **46-47**, 179-182.

Gorecki, C., Jozwik, M. & Salbut, L., *J. Microlith., Microfab., Microsyst.* , 2005, **4 (4)**.

Guy, I.L., Muensit, S. & Goldys, E.M., 1999, *App. Phys. Letters*, **75 (26)**, 4133-4135.

Kim, J.H., Lee, S.H., Ahn, J.H. & Lee, J.K., 2002, *J. Ceramic Processing Research*, **3 (1)**, 25-28.

Kusaka, K., Taniguchi, D., Hanabusa,T. & Tominaga, K., 2000, *Vacuum* , **59**, 806-813.

Lakin, K.M., Belsick, J., McDonald, J.F. & McCarron, K.T., 2001, *IEEE Ultrasonics Symp.*, 3E-5.

Laurent, T., Bastien, F.O., Pommier, J.C., Cachard, A., Remiens, D. & Cattan, E., 2000, *Sensors and Actuators* A, **87**, 26-37.

Löbl, H.P., Klee, M., Wunnicke, O., Kiewitt, R., Dekker, R. & Pelt, E.V., 1999, *IEEE Ultrasonics Symposium*, 1031-1036.

Meng, W.J., Sell, J.A., Eesley, G.L. & Perry, T.A., 1993, *J. Appl. Phys.*, **74 (4)**, 2411-2414.

Oliver, W.C. & Pharr, G.M., 1992, *J. Mater. Res.*, **7**, 1564-1583.

Ruffieux, D., Dubois, M.A. & de Rooij, N.J., 2000, *IEEE MEMS*, 662-667.

Salbut, L., Patorski, K., Jowik, M., Kacperski, J., Gorecki, C., Jacobelli, A. & Dean, T., 2003, *SPIE Proc.* Vol. **5145**, 23-32.

Walter, V., 2001, Thesis université de Franche Comté, Besançon.

Walter, V., Delobelle, P., Le Moal, P., Joseph, E. & Collet, M., 2002, *Sensors and Actuators A,* **96**, 157-166.

Wang, Q.M. & Cross, L.E., 1999, *IEEE Trans. Ultrason., Ferroel. And Freq. Control*, 46 (6), 1343-1351.

Wright, A.F., *J. Appl. Phys*., 1997, **82 (6)**, 2833-2839.